Macromolecules

ARTICLE

pubs.acs.org/Macromolecules

Polylactide−Poly(6-methyl-ε-caprolactone)−Polylactide Thermoplastic Elastomers

Mark T. Martello[‡,§] and Marc A. Hillmyer[*,†,§]

[†]Department of Chemistry, [‡]Department of Chemical Engineering and Materials Science, and [§]Center for Sustainable Polymers, University of Minnesota, Minneapolis, Minnesota 55455-0431, United States

Supporting Information

ABSTRACT: Amorphous ABA type block aliphatic polyesters can be useful as degradable and biorenewable thermoplastic elastomers. These materials can be prepared by sequential ring-opening transesterification polymerization (ROTEP) reactions and can exhibit a range of physical properties and morphologies. In this work a set of amorphous polylactide−poly(6-methyl-ε-caprolactone)−polylactide aliphatic polyester ABA triblock copolymers were prepared by consecutive controlled ring-opening polymerizations. Ring-opening polymerization of neat 6-methyl-ε-caprolactone in the presence of 1,4-benzenedimethanol and tin(II) octoate afforded α,ω-hydroxyl-terminated poly(6-methyl-ε-caprolactone). High conversions of 6-methyl-ε-caprolactone (>96%) afforded polymers with molar masses ranging from 12 to 98 kg mol^{-1}, depending on monomer-to-initiator ratios, polymers with narrow, monomodal molecular weight distributions. An array of polylactide−poly(6-methyl-ε-caprolactone)−polylactide triblock copolymers with controlled molecular weights and narrow molecular weight distributions were synthesized using the telechelic poly(6-methyl-ε-caprolactone) samples as macroinitiators for the ring-opening polymerization of D,L-lactide. The morphological, thermal, and mechanical behaviors of these materials were explored. Several triblocks adopted well-ordered microphase-separated morphologies, and both hexagonally packed cylindrical and lamellar structures were observed. The Flory−Huggins interaction parameter was determined, $\chi(T) = 61.2T^{-1} - 0.1$, based on the order-to-disorder transition temperatures of two symmetric triblocks using the calculated mean field theory result. The elastomeric mechanical behavior of two high molecular weight triblocks was characterized by tensile and elastic recovery experiments.

The commercial success of synthetic polymers rests partly on the availability of inexpensive, nonrenewable petroleum-based feedstocks. However, most of these traditional commodity plastics are destined for environmental persistence. Because of increasing emphasis on sustainability in the polymer industry, great efforts are being made to replace the current polymers with biorenewable and degradable alternatives. Polylactide is a sugar-derived polyester with a hydrolytically degradable backbone[1−3] that has been used in the biomedical industry for degradable devices and more recently in the packaging and textiles industries.[1,4] Amorphous polylactide (PLA) is prepared by the ROTEP of racemic lactide (D,L-lactide). It is a stiff material with a glass-transition temperature (T_g) near 60 °C.[2] Isotactic polylactide is a semicrystalline polymer with a melting temperature (T_m) up to 180 °C. One key to increasing the breadth of PLA applicability is through the controlled incorporation of other components, in particular in the form of block copolymers.[2] Particularly attractive targets are ABA triblock copolymers that incorporate PLA as the end blocks. With appropriate rubbery midblocks, such thermoplastic elastomers (TPEs) can be used in a wide variety of consumer products such as footware, asphalt additives, and hot melt and pressure sensitive adhesives.[5]

Bulk ABA triblocks may adopt well-ordered spherical, cylindrical, gyroid, and lamellar structures that depend on the interaction between A and B repeat units embodied by the Flory−Huggins χ parameter, the total number of repeat units N, and, most importantly, the volume fraction of the components f ($f_A + f_B = 1$).[6] Commercial TPEs such as poly(styrene)-*b*-poly(isoprene)-*b*-poly(styrene) (SIS) typically contain a majority of the rubbery midblock, resulting in dispersed spheres or cylinders of glassy polystyrene that act as physical cross-links for the amorphous, low-T_g matrix.[5] ABA triblocks employing both amorphous PLA and semicrystalline PLLA hard end blocks have been investigated as TPEs. Nondegradable midblocks such as polyisobutylene[7] and poly(dimethylsiloxane)[8] as well as entirely degradable midblocks such as polyisoprene,[9] poly(1,3-trimethylene carbonate) (PTMC),[10] poly(3-hydroxybutyrate),[11] poly(1,5-dioxepan-2-one),[12] and poly(menthide)[13−15] (PM) have been reported. Exchanging amorphous PLA for semicrystalline variants resulted in improved mechanical properties for both PLA−PM−PLA[14] and PLA−PTMC−PLA[10] triblocks; enhanced physical cross-linking due to PLLA crystallite formation has been implicated. However, the ultimate tensile stress of the amorphous triblocks is somewhat low considering the high tensile strength of glassy PLA. Incorporation of crystallizable end blocks in ABA triblocks can present additional challenges due to crystallite formation altering the microstructure and an increased dependence of properties on thermal history.[16−18] For example, triblock PLLA−PTMC−PLLA films formed spherulites after several weeks due to the slow crystallization of the

Received: May 9, 2011
Revised: August 4, 2011
Published: October 14, 2011

Scheme 1

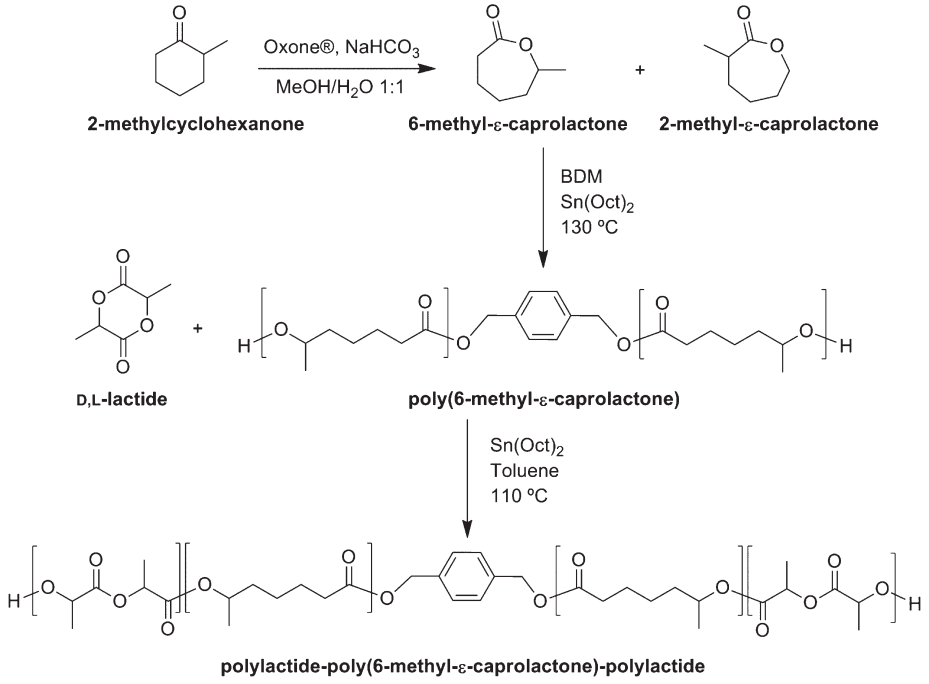

polylactide overriding the initially formed microstructure.[10] Similarly, time dependent analysis of PLLA−PCL diblock copolymers revealed a microphase-separated lamellar morphology upon cooling from the melt that was overwhelmed by PLLA spherulite formation regardless of the composition.[16] Improving the mechanical properties of all amorphous PLA TPEs could significantly improve their applicability and thus expand their range of applications.

We report the synthesis and properties of amorphous PLA−poly(6-methyl-ε-caprolactone)−PLA (L−MCL−L) triblocks. We utilized a new Baeyer−Villiger protocol for the preparation of MCL from 2-methylcyclohexanone. The polymerization of 6-methyl-ε-caprolactone (MCL) has been previously reported using tin, aluminum, and enzymatic catalysts.[19−25] This is the first report using poly(6-methyl-ε-caprolactone) (PMCL) in a block copolymer. PMCL is an amorphous polymer exhibiting a low T_g (−45 °C). On the basis of previous works with ε-caprolactone[16] (CL) and (−)-menthide,[15] we anticipated that MCL and LA would be sufficiently incompatible that microphase separation could be achieved at convenient molar masses. Symmetric hydroxyl-terminated PMCL prepolymers were prepared and subsequently used as macroinitiators for the ROTEP of D,L-lactide to form amorphous PLA−PMCL−PLA triblocks. The parameters dictating the self-assembly behavior and the microstructure of the triblock copolymers were established. In addition, the mechanical properties were analyzed and correlated with the overall molar mass of the triblocks.

RESULTS AND DISCUSSION

Synthesis of 6-Methyl-ε-caprolactone. We employed the Baeyer−Villiger (BV) oxidation of 2-methylcyclohexanone for the preparation of MCL. Oxone (ca. 2 equiv of $KHSO_5$) was added to a solution of 2-methylcyclohexanone in methanol/water (1:1 v/v) containing excess sodium bicarbonate to mitigate the acidity of the reaction mixture.[26] The insoluble salts were filtered, and the resulting solution was extracted with dichloromethane to give MCL in quantitative yield. The product was purified by fractional distillation and analyzed by ^{1}H and ^{13}C NMR spectroscopies. The monomer characterization data were consistent with previous reports[27] and contained 5% of the regioisomer 2-methyl-ε-caprolactone (2-MCL). A representative ^{1}H NMR spectrum is given in Figure S1. The concentration of 2-MCL did not change upon purification, and the mixture of isomers was used in subsequent polymerizations. We refer to the mixture of 6-MCL and 2-MCL isomers as MCL. Prior to polymerization, the monomer was passed through a column of activated basic alumina to remove any residual water or trace impurities.

The use of Oxone as a replacement for more hazardous oxidants such as *m*-chloroperbenzoic acid and trifluoroperacetic acid has been investigated due to both environmental and safety concerns.[28−30] This powerful oxidant has seen little use for the preparation of strained lactones due to (catalyzed) hydrolysis of the desired product.[28,29] Oxone has not been widely used in anhydrous organic solvents due to its poor solubility. Additionally, 2-methylcyclohexanone is insoluble in water. There has been recent effort on increasing the availability of Oxone under anhydrous conditions by preloading the oxidant on a solid support such as silica,[28,29] although the supported oxidant shows a loss of reactivity if it is not stored at 2 °C.[28] In this work, a solvent mixture of water and methanol was employed, but sodium bicarbonate was added to the reaction to moderate the acidity of the reaction mixture. Although the limited solubility of sodium bicarbonate and Oxone in the methanol/water mixture could potentially limit the efficiency of the reaction, the high yields of MCL obtained after extraction indicate that the partial solubility of these reagents is sufficient. This simple procedure to prepare MCL offers many advantages compared to more conventional BV techniques.

Synthesis and Characterization of HO−PMCL−OH. The polymerization of MCL was carried out in the bulk at 110 or

Table 1. Ring-Opening Polymerization of 6-Methyl-ε-caprolactone

						M_n (kg/mol)			
sample	$[M]_0/[I]_0$	$[M]_0/[Sn]_0$	time (h)	temp (°C)	conv (%)	theor[a]	NMR[b]	SEC	PDI
PMCL-12	95.4	374	7.8	110	99	12.1	11.9	25.2	1.15
PMCL-16	131	398	7.8	110	98	16.5	16.0	32.2	1.15
PMCL-20	156	500	16	110		20.0[c]	20.2	43.6	1.19
PMCL-41	318	482	6.0	130	96	39.1	41.1	59.7	1.18
PMCL-73	518	462	8.3	130	100	66.4	72.9	146	1.23
PMCL-98	780	794	8.2	130	85	85.0	98.4	153	1.22

[a] Theoretical M_n was calculated based on the observed monomer conversion (p) and the initial monomer and initiator content, $M_n = M_0 \times p \times [M]_0/[I]_0$. [b] Molecular weight calculated from end-group analysis (BDM). [c] Theoretical M_n based on 100% conversion as the conversion data were not obtained.

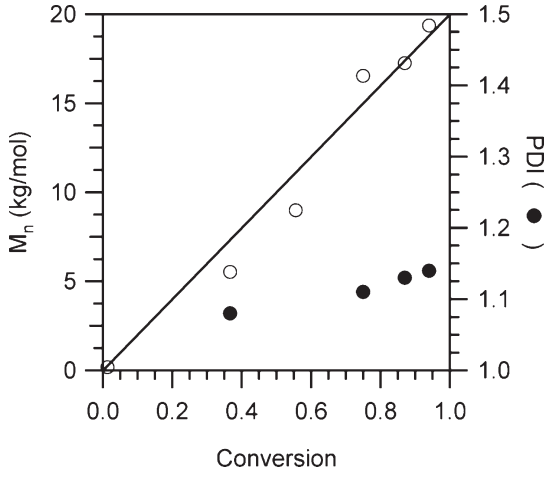

Figure 1. Dependence of number-average molecular weight determined by ^{1}H NMR spectroscopy (○) and polydispersity index (●) determined by SEC on MCL conversion. The theoretical molar mass is indicated by the solid line. The polymerization was carried out at 130 °C in the bulk with a monomer-to-catalyst ratio of 503 and a monomer-to-initiator ratio of 156.

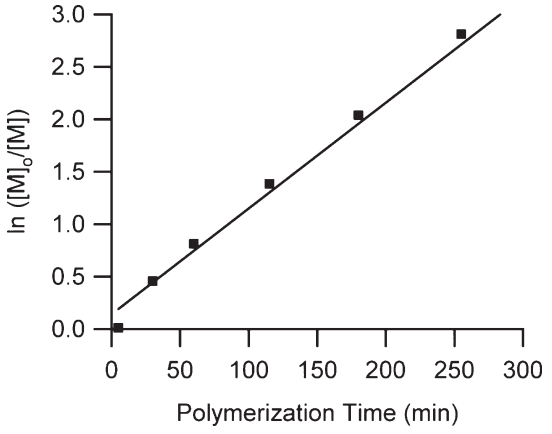

Figure 2. MCL consumption as a function of time determined by ^{1}H NMR spectroscopy. The polymerization was carried out at 130 °C in the bulk with a monomer-to-catalyst ratio of 503 and a monomer-to-initiator ratio of 156.

130 °C using 1,4-benzenedimethanol (BDM) as a difunctional initiator and tin(II) ethylhexanoate ($Sn(Oct)_2$) as the catalyst (Scheme 1). A series of six polymerizations with [MCL] to [BDM] ratios ranging from 95 to 780 were investigated (Table 1). An aliquot of the cooled reaction mixture was analyzed by ^{1}H NMR spectroscopy. Proton(s) α to the acyl oxygen in the polymer backbone for 6-MCL and 2-MCL repeat units appear at δ = 4.9 ppm and δ = 4.1 ppm, respectively (Figure S2). Monomer conversion calculated from the integral ratio of the monomer and repeat units was typically greater than 96% and up to 99%. The relative integration of the 6-MCL and 2-MCL repeat units in the polymer closely matched the ratio in the feed (5% 2-MCL), indicating that both isomers are incorporated into the polymer chain. Incorporation of the BDM initiator is supported by the quantitative shift of the benzylic protons from δ = 4.7 ppm to δ = 5.1 ppm upon conversion of the alcohol to the corresponding ester. After precipitation of the polymer, the molar mass characteristics were determined by SEC using polystyrene standards (Table 1). The M_n determined by SEC was higher than the predicted value based on the monomer-to-initiator ratio and the monomer conversion as determined by ^{1}H NMR spectroscopy. The monomodal molar mass distributions gave low polydispersity indices close to 1.2 in all cases. The methine proton corresponding to the hydroxyl chain end was observed at δ = 3.8 ppm, and end-group analysis was used to calculate M_n assuming exactly one BDM moiety per chain. The measured value of M_n was consistent with the theoretical M_n based on monomer conversion and the initial ratio of monomer and BDM (Table 1). The integration ratio of these methine end group protons to the benzylic methylene resonances from the BDM was close to 2, indicating adventitious initiation (e.g., by water) was suppressed.

Several reaction aliquots from a bulk MCL polymerization at 130 °C were analyzed by ^{1}H NMR spectroscopy and SEC. Shown in Figure 1, the molecular weights determined by ^{1}H NMR spectroscopy increased linearly with conversion while the PDI values showed only modest increases over the same time frame. The rate of polymerization was first order in MCL concentration, evident by the linear relationship observed in Figure 2. Assuming first-order catalyst dependence, we observe a second-order rate constant of 0.012 M^{-1} s^{-1} at a bulk catalyst concentration of $[Sn(Oct)_2] = 15.6 \times 10^{-3}$ mol kg^{-1} (assuming a constant density of 1 kg L^{-1}). Storey and Sherman reported the bulk polymerization of ε-caprolactone (CL) catalyzed by $Sn(Oct)_2$ ($[Sn(Oct)_2] = 1.2 \times 10^{-3}$ mol kg^{-1}) at 130 °C reached 95% conversion after 40 min.[31] At $[Sn(Oct)_2] = 15.6 \times 10^{-3}$ mol kg^{-1}, MCL reaches 95% conversion after 255 min. The difference in rates is likely due to the steric hindrance around the

Table 2. Characteristics of L−MCL−L Triblock Copolymers

			SEC				
sample	wt % PLA[a]	f_{PLA}[b]	M_n (kg/mol)	PDI	$T_{g(MCL)}$ (°C)	$T_{g(PLA)}$ (°C)	morph
L−MCL−L (4.6−20−4.6)	31	0.26	49	1.18	−43	29	
L−MCL−L (6.7−20−6.7)	39	0.33	53	1.16	−43	36	cylinder
L−MCL−L (7.1−21−7.1)	41	0.35	52	1.08	−42	38	cylinder
L−MCL−L (13−20−13)	58	0.52	52	1.19	−44	42	
L−MCL−L (20−20−20)	69	0.63	67	1.40	−55	33	lamellar
L−MCL−L (30−20−30)	73	0.72	97	1.35	−44	48	lamellar
L−MCL−L (7−12−7)	55	0.49	44	1.11	−41	39	lamellar
L-MCL-L (9.6−16−9.6)	55	0.49	49	1.17	−42	43	lamellar
L−MCL−L (26−38−26)	58	0.52	110	1.18	−45	50	lamellar
L−MCL−L (12−98−12)	20	0.16	172	1.18	−43	50	
L−MCL−L (25−98−25)	34	0.29	195	1.22	−43	52	

[a] Mass percent PLA determined by ^{1}H NMR spectroscopy. [b] Calculated volume fraction PLA assuming 25 °C with pure component densities: ρ_{PLA} = 1.25 g cm^{-3} and ρ_{PMCL} = 0.98 g cm^{-3}.[37]

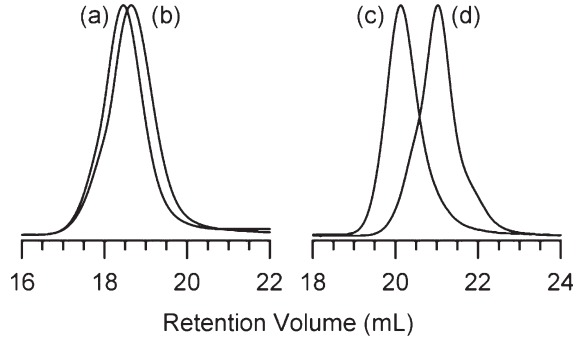

Figure 3. SEC traces of (a) L−MCL−L (12−98−12), (b) PMCL (98), (c) L−MCL−L (7−12−7), and (d) PMCL (12).

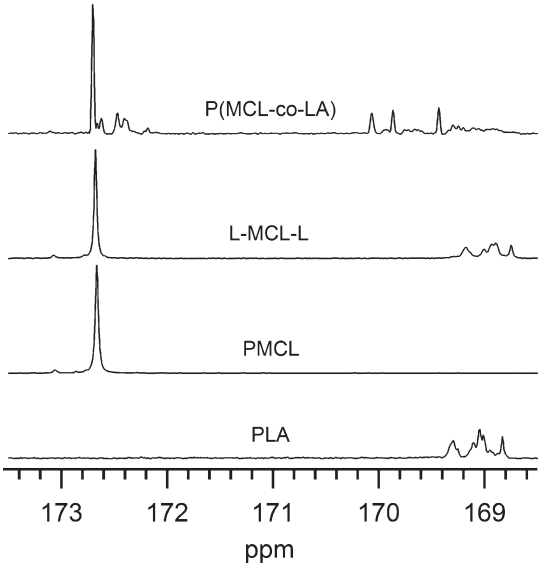

Figure 4. ^{13}C NMR spectra of PLA, PMCL, L−MCL−L triblock, and poly(MCL-*s*-LA).

ester group imposed by the methyl group in MCL.[32] This result is consistent with the work of Vion et al.,[25] who reported rate constants of 4.05 and 0.035 M^{-1} s^{-1} for CL and MCL, respectively, using Al(*i*PrO)$_3$ in toluene at 25 °C ([CL or MCL]$_0$ = 1 M and [Al(*i*PrO)$_3$] = 5 mM). The high conversion of MCL (Table 1) at 130 °C suggests that the methyl substitution does not significantly decrease the ring-strain when compared to CL.

Synthesis and Characterization of PLA−PMCL−PLA. L−MCL−L triblocks were prepared in toluene at 110 °C using α,ω-dihydroxyl telechelic PMCLs as macroinitiators and Sn(Oct)$_2$ as the catalyst for the ring-opening polymerization of D,L-lactide (Table 2). The precipitated polymers were analyzed by ^{1}H NMR spectroscopy and SEC. The methine proton associated with the PMCL hydroxyl terminus was absent upon chain extension and the terminal LA methine proton appeared at δ = 4.4 ppm, indicating quantitative initiation efficiency (see Figure S3). The relative integration of the benzyl protons in the PMCL initiator fragment to the terminal PLA methine protons was close to 2, indicating high reinitiation efficiency. A value larger than 2 would indicate the presence of excess PLA homopolymer as a result of initiating impurities being introduced to the reaction. The methine protons of the LA repeat unit (δ = 5.2 ppm) was used to calculate the weight fraction of PLA in the triblock. The observed triblock composition was in good agreement with the weight fraction of D,L-lactide in the feed after accounting for lactide conversion. Comparison of representative MCL prepolymer and L−MCL−L triblock SEC chromatograms is shown in Figure 3. The observed shift to shorter retention times is consistent with the desired chain extension reaction. In agreement with the ^{1}H NMR results, these data support the conclusion that the triblocks are relatively free of PLA homopolymer (Table 2).

By employing a sequential ROTEP scheme to prepare an aliphatic polyester block copolymer, a chain transfer process can occur whereby the active chain end of a PLA block can undergo a transesterification reaction with the PMCL midblock liberating an MCL chain end. This process would lead to a randomization of the chain sequence and compromise the desired ABA architecture. The absence of the MCL chain ends in the triblock ^{1}H NMR spectra supports limited or no transesterification during the triblock synthesis. The sequence distribution of polyester copolymers can be investigated by examining the carbonyl carbon

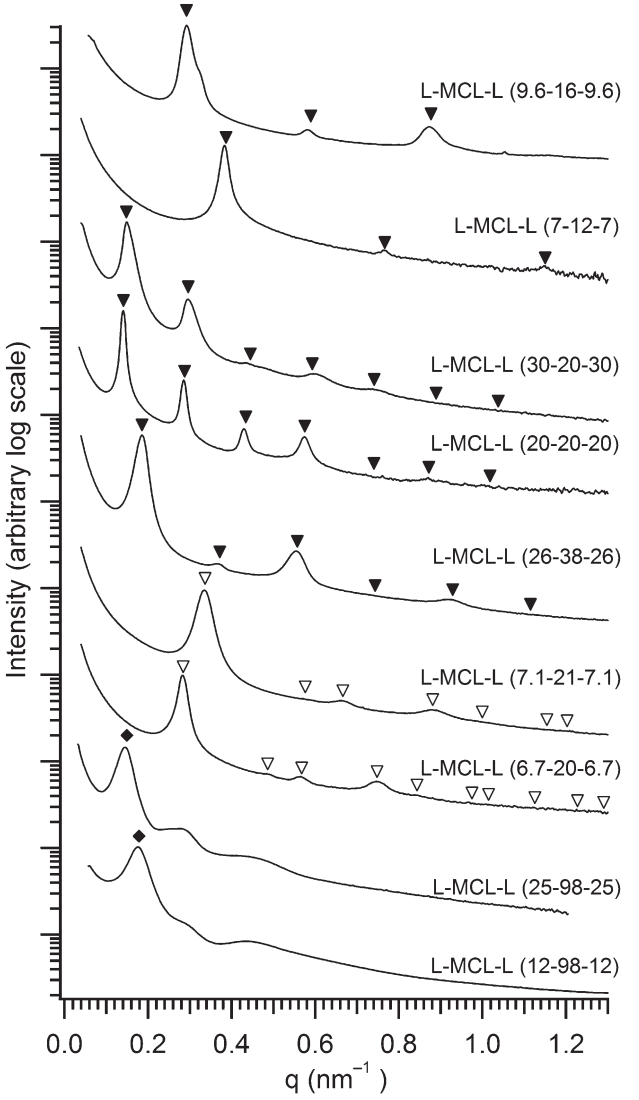

Figure 5. Small-angle X-ray scattering of L−MCL−L triblocks at room temperature. L−MCL−L (7−12−7) was analyzed at 100 °C. The Bragg reflections for identified lamellar (▼) and cylindrical (▽) morphologies are indicated above each trace. The primary peak positions for L−MCL−L (25−98−25) and L−MCL−L (12−98−12) are indicated with diamonds (◆).

(C═O) region of the ^{13}C NMR spectrum, as the carbonyl ^{13}C signal is sensitive to the microstructure of the copolymer. In Figure 4, the ^{13}C NMR spectrum in the region of δ = 168−174 ppm is shown for representative PMCL, PLA, L−MCL−L, and poly(MCL-*s*-LA). The C═O resonances of homopolymer PLA were observed between 168.9 and 169.6 ppm,[33] and for PMCL a resonance at 172.6 ppm was observed; the small peak near 173.1 ppm corresponds to the 2-MCL repeat unit. The statistical copolymer poly(MCL-*s*-LA) was synthesized by adding both MCL and lactide monomers at the start of the polymerization in the molar ratio of 2:1, respectively. Notably, the additional resonances observed in poly(MCL-*s*-LA) are absent in the L−MCL−L triblock spectrum. These additional peaks are a result of the monomer sequence generated from the cross-propagation reactions between lactide and MCL active chain ends with both MCL and lactide. On the basis of the LA and CL copolymerization behavior,[34] we would expect the copolymerization of MCL and lactide to form a "blocky" structure of alternating PLA

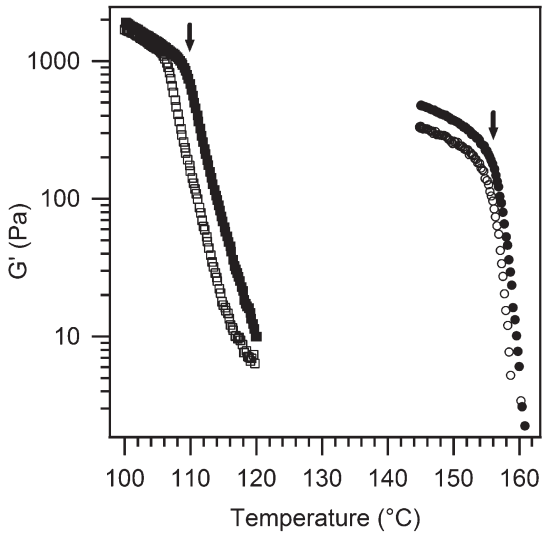

Figure 6. Isochronal temperature sweep of L−MCL−L (7−12−7) upon heating (■) and cooling (□) and L−MCL−L (9.6−16−9.6) on heating (●) and cooling (○).

and PMCL sequences. Without MCL monomer present during the polymerization, transesterification between the PLA and PMCL blocks is the only plausible mechanism that could generate alternating sequences. The absence of these signals in the L−MCL−L triblock ^{13}C NMR spectrum indicates the PLA chain end does not react with the PMCL backbone. Our results are consistent with previous reports where transesterification between block polyesters is absent for Sn(Oct)$_2$-catalyzed polymerization of LA initiated by prepolymers of PCL[35] and poly(menthide)[13] even at long reaction times. The minimum LA reaction times needed to reach high conversion were used to avoid broadening of the molecular weight distribution in the PLA blocks which has been shown to influence the domain spacing and equilibrium morphology.[36]

Small-Angle X-ray Scattering (SAXS). The morphology of L−MCL−L triblocks were analyzed by SAXS at room temperature (Figure 5). L−MCL−L (6.7−20−6.7) and L−MCL−L (7.1−21−7.1) showed well-defined principal reflections with higher order reflections allowed by the *p6mm* space group (▽ annotation in Figure 5).[6] Hexagonally packed PLA cylinders within a PMCL matrix is consistent with this scattering and compositions of these two samples (39−41 wt %).[6] Triblocks with increased PLA content, 55−69 wt % PLA, showed higher order reflections at integral multiples (▼ annotation in Figure 5) of q/q^*, indicating a lamella microstructure. For L−MCL−L (26−38−26) low-intensity reflections at $2q^*$, $4q^*$, and $6q^*$ were observed, suggesting a symmetric lamellar structure. The high molecular weight triblocks L−MCL−L (12−98−12) and L−MCL−L (25−98−25) showed a pronounced principal reflection followed by broad oscillations in intensity at higher q. The anticipated morphology of L−MCL−L (12−98−12) is PLA spheres dispersed in a PMCL matrix.[6] This was investigated by comparing the observed scattering profile to the dispersed sphere form factor model (Figure S4). Using a sphere radius of 21.5 nm, the simulated form factor scattering profile is in good agreement with the features observed experimentally. On the basis of composition of L−MCL−L (25−98−25), we anticipate a cylindrical morphology where PLA cylinders are dispersed in a PMCL matrix (see Figure S5). We believe this sample adopts microphase-separated structure, but long-range ordering is prevented

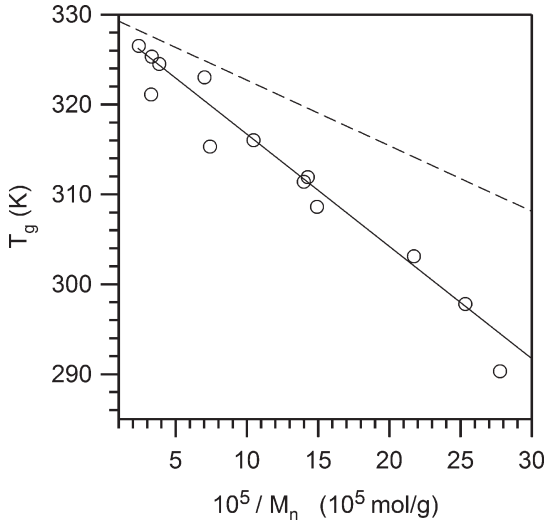

Figure 7. Molar mass dependence of the PLA domain glass transition temperature in bulk L−MCL−L triblocks. The ordinate is inverse molecular weight of the PLA block length. The solid line is the Flory−Fox fit (eq 3) for the L−MCL−L triblocks, and the dashed line is Flory−Fox dependence of homopolymer PLA reported by Jamshidi et al.[45]

due to slow equilibration kinetics at this molar mass and degree of segregation (see below); thus, the scattering is less well-resolved in this case.[38,39]

PMCL−PLA χ Parameter. Order−disorder transition temperatures (T_{ODT}) were determined by dynamic mechanical spectroscopy and SAXS for two lamellar triblocks: L−MCL−L (7−12−7) and L−MCL−L (9.6−16−9.6). The dynamic mechanical moduli were measured at a heating rate of 1 °C/min.[40] Strain sweep experiments were conducted to ensure the temperature ramps were conducted within the linear viscoelastic limit (Figure S6). T_{ODT} values were determined from the midpoint of the discontinuous drop in G'. Shown in Figure 6, G' for L−MCL−L (7−12−7) decreases rapidly as the sample is heated above 115 °C (T_{ODT}). The transition is also thermally reversible upon cooling. This value for T_{ODT} was corroborated by SAXS data taken at 10 °C intervals that revealed a discontinuous drop in intensity and broadening of the principal reflection between 110 and 120 °C (see Figure S7). Similarly, L−MCL−L (9.6−16−9.6) disorders at 155 °C.

Mean-field theory calculations give the position of the lamellar/disorder phase boundary at $\chi(T_{ODT}) = 18\ N^{-1}$ for ABA triblocks with equal A and B volume fractions. In this work we assume χ is dependent on temperature given according to eq 1.

$$\chi(T) = \frac{a}{T} - b \tag{1}$$

The overall degree of polymerization, N, was calculated based on a standard reference volume of 118 Å^3 using the room temperature densities of the respective homopolymers.[41] Based on the measured order-to-disorder transitions, χ for the PLA−MCL (χ_{L-MCL}) system is given by eq 2.

$$\chi(T) = \frac{61.2}{T} - 0.1 \tag{2}$$

For comparison, the values of χ at 140 °C and a segment volume of 118 Å^3 for other pairs of polymers common to block copolymers are PS/PI = 0.04,[42] PMCL/PLA = 0.05, PS/PLA = 0.08,[43] and PEP/PLA= 0.29[44] (PS, PI, and PEP refer to polystyrene, polyisoprene, and poly(ethylene-*alt*-propylene, respectively.)

Table 3. Tensile Properties of Selected L−MCL−L Samples at Room Temperature

sample	wt % PLA	E (MPa)	σ_b (MPa)	ε_b (%)	ε_{resid} (%)
L−MCL−L (12−98−12)	20	1.87 ± 0.03	10.2 ± 0.8	1880 ± 70	2−4
L−MCL−L (25−98−25)	34	31 ± 9	14.2 ± 1.9	1360 ± 120	4−6

Thermal Analysis. Analysis of the bulk triblock copolymers by differential scanning calorimetry revealed two glass transition temperatures with no evidence of crystallization. Representative thermograms are shown in Figure S9. We attribute the observed glass transitions to PMCL- and PLA-rich domains. The glass transition of the MCL block appeared at −45 °C and was relatively invariant over the molecular weight and compositions studied. The glass transition temperatures for the PLA block, however, showed a strong dependence on the PLA block molecular weight and ranged from 17 to 55 °C. The molecular weight dependence between 3.6 and 42 kg mol^{-1} for PLA was analyzed according to the Flory−Fox equation:

$$T_g = T_g^{\infty} - \frac{K}{\bar{M}_n} \tag{3}$$

where T_g^{∞} is the T_g of the polymer at infinite molecular weight and K is a constant representing the excess free volume of the end groups. As shown in Figure 7, the temperature dependence of the PLA T_g is well represented by the Flory−Fox equation with T_g^{∞} = 53 °C and $K = 1.12 \times 10^5$.

Partial mixing of PMCL in the PLA domain could lower T_g value compared PLA homopolymer of comparable molar mass. To facilitate comparison with homopolymer PLA, a line (dashed) generated from the Flory−Fox parameters reported by Jamshidi et al.[45] (T_g^{∞} = 57 °C and $K = 7.30 \times 10^4$) is included in Figure 7. The highest T_g observed in L−MCL−L triblocks was 53 °C (41 kg mol^{-1}), which is ∼5 deg lower than comparable homopolymer PLA. With decreasing molecular weight the deviation from homopolymer PLA increases. Similar behavior has been reported for styrenic block copolymers containing poly(dimethylsiloxane)[46−48] or poly(butadiene),[49] where the polystyrene T_g in the block copolymer is lower than the homopolymer equivalent at low to moderate molar masses. The block and homopolymer polystyrene T_gs were found to converge at polystyrene block M_n of 1.8 and 70 kg mol^{-1} for poly(dimethylsiloxane) and poly(butadiene) block copolymers, respectively. This difference was attributed to the relative compatibility of each system. Comparing the two systems, Granger et al. noted that the segregation strength (χN) did not quantitatively correlate with the critical molar mass observed for the two systems; however, a quantitative agreement was achieved using $\chi^2 N$.[49] Their empirical observation implies an increased χ dependence which could also explain why the T_g^{∞} of PLA in the L−MCL−L triblocks is lower than homopolymer PLA since $\chi_{PLA-PMCL}$ is on the order of χ_{PS-PI}.

Tensile Properties. The tensile properties of two high molecular weight triblocks, L−MCL−L (12−98−12) and L−MCL−L (25−98−25), were evaluated (Table 3). Although the samples were tested to their breaking points, the failures occurred at the grips and not in the gage; thus, the ultimate stress and strain values reported are likely underestimates. The change in the sample thickness at the high elongations required overtightening

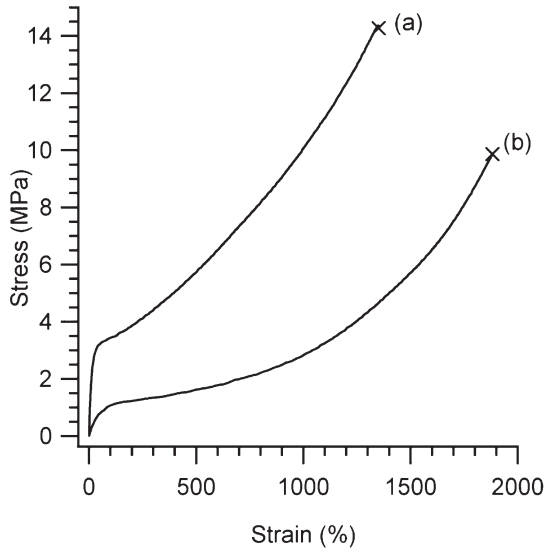

Figure 8. Representative stress−strain curves of (a) L−MCL−L (25−98−25) and (b) L−MCL−L (12−98−12) triblocks. Experiments were conducted at room temperature and 15 cm min^{-1}. The point of failure is indicated by ×.

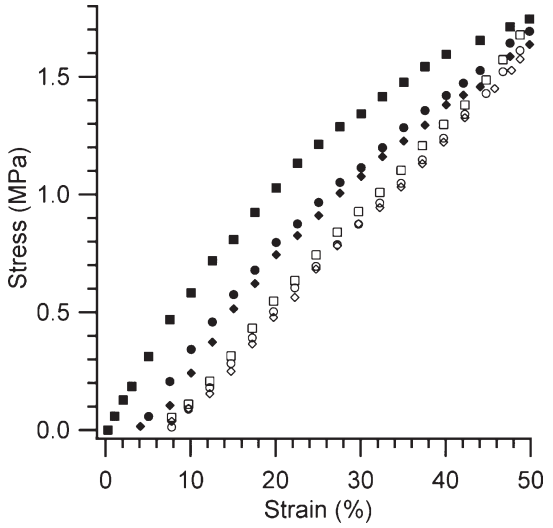

Figure 9. Reciprocating tensile properties of L−MCL−L (25−98−25) from 0 to 50% strain at ±5 mm min^{-1} for 20 cycles. The closed symbols represent the sample upon extension and the open symbols on retraction for cycles 1 (■), 2 (●), and 20 (◆).

the grips to avoid the sample slipping in the grips.[50] Representative engineering stress−strain curves for each triblock are given in Figure 8. Notably, both L−MCL−L triblocks reach strains in excess of 1000% prior to failure. Increasing the PLA content from 20 and 34 wt % results in a 17-fold increase in Young's modulus, a 40% increase in the stress at break, and a 25% decrease in the strain at break.[51] Understanding the deformation mechanisms associated with these materials, such as chain pullout[52] and alignment of the microstructure,[9,53−55] could potentially guide future efforts to maximize the toughness of these triblocks.

The tensile testing of previously reported amorphous polyester PLA−PM−PLA triblocks with 32 and 42 wt % PLA gave tensile strengths of 3.8 and 3.7 MPa and strains at break of 872 and 530%, respectively.[14,15] The L−MCL−L triblocks in this report have molecular weights approximately 2−3-fold larger than the PLA−PM−PLA triblocks with comparable PLA T_g values (∼50 °C). The improvement in tensile strength and elongation for L−MCL−L samples is most likely due to the increased molecular weight of the PLA end blocks.[53,54] Alternatively, the ultimate strength of ABA triblocks has also been related to the entanglement molecular weight of the midblock,[55] which may be responsible for the observed differences between PM and PMCL containing samples. Compared to commercially available styrenic block copolymers, the molecular weight and composition are similar, but the ultimate tensile stresses are notably smaller by factors of 2−4.[5]

Select L−MCL−L samples were also subjected to 20 cycles of 50% reciprocating strain at a constant rate of displacement of 5 mm/min. Comparison of the stress−strain profiles between cycles indicates the level of plastic deformation that occurred between cycles. Figure 9 shows the stress−strain behavior of L−MCL−L (25−98−25) for cycles 1, 2, and 20. After the first cycle, there is a modest reduction of the extensional engineering stress at constant strain levels for cycle 2; however, for cycles 3−20 the stress−strain behavior was nearly identical. L−MCL−L (12−98−12) exhibited a higher level of recovery between the first and second cycle and almost no change between cycle 2 and 20 (see Figure S10). The initial plastic deformation may be attributed to the alignment of the microstructure.[9,56−58] The residual strain (ε_R) values, reported in Table 3, indicate these materials have a high level of recovery when subject to 50% strain.

■ CONCLUSIONS

We have demonstrated a simple procedure for the preparation of amorphous L−MCL−L aliphatic polyester triblocks. Additionally, a Baeyer−Villiger protocol that uses non-chlorinated solvents with higher atom economy was developed for the synthesis of MCL in high yield. The bulk polymerization of MCL was well controlled, enabling the preparation of polymers with targeted molar masses and low polydispersity indices. Well-defined L−MCL−L triblocks were prepared from a sequential ring-opening polymerization scheme using a commercially available $Sn(Oct)_2$ catalyst. The composition of the triblocks was in good agreement with the feed composition. The bulk triblock properties were investigated using DSC, SAXS, DMA, and tensile experiments. An array of L−MCL−L triblocks were microphase separated according to both SAXS, DSC, and DMA data. Ordered cylindrical and lamellar morphologies were also observed in the one-dimensional SAXS profiles. The Flory−Huggins interaction parameter was determined from order-to-disorder transition temperatures for two symmetric L−MCL−L triblocks. The glass transition of the PLA domain in the microphase-separated triblocks showed Flory−Fox type behavior based on the PLA block molar mass. In the range of molar masses studied the PLA T_g appears lower than its homopolymer equivalent. Analysis of the L−MCL−L triblocks was concluded with select tensile properties demonstrating elastomeric behavior with exceptional elongation and tensile strength. The combined properties of the L−MCL−L triblocks are promising for engineering degradable thermoplastic elastomers and related materials.

■ EXPERIMENTAL SECTION

Materials. Tin(II) 2-ethylhexanoate (Sigma-Aldrich) was distilled (3×) under reduced pressure and stored under an N_2 environment. 1, 4-Benzenedimethanol (Sigma-Aldrich) was dried under reduced pressure at room temperature for 48 h. Toluene was purified by passing

though activated alumina columns (Glass Contour, Laguna Beach, CA) prior to use. D,L-Lactide (Purac) was recrystallized (2×) from toluene and dried under vacuum. Toluene, $Sn(Oct)_2$, BDM, MCL, and LA were stored and handled in a nitrogen environment (glovebox). Glass pressure vessels, Teflon caps, and Teflon-coated magnetic stir bars were stored in a 110 °C oven prior to being transferred to the glovebox. All other solvents were used as received without further purification.

Characterization. ^{1}H NMR spectra were collected from $CDCl_3$ solution on a Varian INOVA-500 spectrometer operating at 500 MHz. ^{13}C NMR spectra were collected at 126 MHz. Chemical shifts are reported in δ (ppm) relative to the ^{1}H signals from the protic solvent (7.26 ppm for $CHCl_3$). Size-exclusion chromatography (SEC) was conducted on a liquid chromatograph (Agilent 1100 series) equipped with a HP1047A refractive index detector. Polymer samples were diluted in $CHCl_3$ (mobile phase) and passed through three Varian PLgel Mixed C columns at 35 °C under a constant volumetric flow rate (1 mL min^{-1}). Molecular weight characteristics of the samples are referenced to polystyrene standards (Polymer Laboratories). Small-angle X-ray scattering experiments were conducted at Argonne National Laboratories in Sector 5-ID-D maintained by the Dow−Northwestern−Dupont Collaborative Access Team (DND-CAT). The X-ray wavelength was 0.73 Å, and the sample-to-detector distance was 6.52 m. The detector was a Mar CCD area detector with a 165 mm diameter. Differential scanning calorimetry was conducted on a TA Instruments Q-1000 DSC. Samples were analyzed in hermetically sealed aluminum pans. The samples were equilibrated at 100 °C and cooled to −100 at 10 °C min^{-1} followed by heating to 100 at 10 °C min^{-1}. Glass transitions are reported upon the second heating cycle. Tensile testing was conducted at room temperature on a Rheometrics Scientific MiniMat instrument. Samples were prepared by pressing the polymer between Teflon sheets in a thermostated press (140 °C) to form a uniform sheet thickness (∼0.18 mm). Dog-bone-shaped samples were cut using a die for a gauge length of 10 mm and width of 3.3 mm. Uniaxial extension was conducted at 5 mm min^{-1}. The order−disorder transition temperatures (T_{ODT}) were determined by dynamic mechanical analysis was conducted on a Rheometrics Scientific AR-G2 stress controlled instrument between 25 mm parallel plates at an angular frequency of 1 rad/s. Dynamic strain sweeps were conducted at temperatures near the T_{ODT} to ensure the measurements were in the linear regime (Figure S6).

6-Methyl-ε-caprolactone (MCL). Synthesis of 6-methyl-ε-caprolactone was prepared from 2-methylcyclohexanone (Aldrich) using Oxone as the oxidant. To a 100 mL round-bottom flask 2-methylcyclohexanone (0.721 g), methanol (20 mL), water (20 mL), and sodium bicarbonate (3 g) were added. The vessel was vigorously stirred with a Teflon-coated magnetic stir bar. Oxone (4 g) was added in two portions —the second added 10 min after the first. After the addition of Oxone (ca. 2 equiv of $KHSO_5$) vigorous gas evolution occurred over 20 min, abated, and ceased after ∼1 h. The reaction was allowed to stir for 6 h followed by filtration and was then extracted with methylene chloride. The organic phase was concentrated under vacuum. A total of 0.82 g was recovered for a quantitative yield. The monomer was purified by fractional vacuum distillation (the distillate temperature was 55 °C at 0.98 Torr) from calcium hydride and stored over 3 Å activated molecular sieves. Additional purification of 6-methyl-ε-caprolactone was needed to produce monomodal high molecular weight PMCL by passing the distilled monomer through a column of activated alumina under nitrogen. ^{1}H NMR ($CDCl_3$): δ 4.4 (m, 1H), 4.2 (m, 0.07H), 2.58 (m, 2H), 1.85 (m, 3.14H), 1.54 (m, 3.28H), 1.29 (d, J = 6.4 Hz, 3H), 1.13 (d, J = 6.7 Hz, 0.12H). ^{13}C NMR ($CDCl_3$): δ 176, 76.9, 36.2, 35.1, 28.3, 22.9, 22.7.

Synthesis of PMCL-16. The following is a typical procedure for the preparation of poly(6-methyl-ε-caprolactone) (PMCL). In the glovebox $Sn(Oct)_2$ (0.0398 g, 98 μmol), BDM (0.0412 g, 0.30 mmol), and MCL (5 g, 39.1 mmol) were added to a 15 mL pressure vessel equipped with a Teflon-coated magnetic stirbar. The sealed reaction vessel was placed in a 110 °C oil bath and stirred for 8 h. The cooled reaction solution was diluted with ∼10 mL of tetrahydrofuran and precipitated into hexanes. The solvent was removed under reduced pressure at room temperature for 3 days. ^{1}H NMR ($CDCl_3$): δ 7.32 (s, 4H), 5.1 (s, 4H), 4.86 (m, 120H), 4.02 (t, J = 6.1 Hz, 9H), 3.77 (m, 2H), 2.24 (t, J = 7.3 Hz, 242H), 1.51−1.67 (br, 398H), 1.4−1.51 (br, 135H), 1.22−1.38 (br, 273H), 1.17 (d, J = 6.1 Hz, 383H). ^{13}C NMR ($CDCl_3$): δ 173, 70.1, 35.2, 34.1, 24.5, 24.4, 19.6.

Synthesis of L−MCL−L (9.6−16−9.6) Triblock Copolymer. In the glovebox PMCL-16 (0.8719 g), $Sn(Oct)_2$ (0.006 g, 1.5 μmol), D,L-lactide (1.0623 g), and toluene (5 g) were added to a 15 mL pressure vessel equipped with a Teflon-coated magnetic stirbar. The sealed reaction vessel was placed in a 110 °C oil bath and stirred for 2 h. The reaction solution was cooled to room temperature and precipitated in methanol (Sigma-Aldrich). The solvent was removed under reduced pressure at room temperature for 3 days. ^{1}H NMR ($CDCl_3$): δ 7.35 (s, 4H), 5.12−5.4 (br, 234H), 5.1 (s, 5H), 4.9 (m, 120H), 3.36 (m, 2.5H), 4.04 (t, J = 6.1 Hz, 9H), 2.27 (t, J = 7.55 Hz, 228H), 1.53−1.75 (br, 1093H), 1.45−1.53 (br, 152H), 1.26−1.42 (br, 251H), 1.2 (d, J = 6.3 Hz, 348H). ^{13}C NMR ($CDCl_3$): δ 173, 169, 70, 68.6, 35.1, 34.1, 24.6, 24.5, 19.6, 16.3.

Kinetics Experiment. MCL polymerization ([MCL]:[BDM]:[$Sn(Oct)_2$] = 156:1:0.31 mol) was carried out at 130 °C in the bulk and studied by removing aliquots as the reaction progressed. To facilitate sampling of the viscous polymer, a three-neck round-bottom flask was equipped with an overhead stirrer, a N_2 inlet valve, and a removable stopper. Samples were taken periodically by temporarily opening the reactor under a high flow of nitrogen and removing an aliquot. Time zero was taken as the time the reaction was placed in the oil bath, and the first value of conversion at 5 min is thus anomalously low. Reactor headspace was purged with nitrogen and sealed after each sample was taken. Reaction aliquots were quickly transfer into sealed scintillation vials and temporarily stored over dry ice to prevent any further reaction. For analysis the samples were warmed to room temperature, diluted, and analyzed immediately. Monomer conversion and M_n were calculated using ^{1}H NMR spectroscopy. Molecular weight and PDI were calculated from SEC analysis referenced to polystyrene standards.

■ ASSOCIATED CONTENT

Supporting Information. Figures S1−S10. This material is available free of charge via the Internet at http://pubs.acs.org.

■ AUTHOR INFORMATION

Corresponding Author
*E-mail: hillmyer@umn.edu.

■ ACKNOWLEDGMENT

SAXS data were acquired at the DuPont−Northwestern−Dow Collaborative Access Team (DND-CAT) located at Sector 5 of the Advanced Photon Source (APS). DND-CAT is supported by I.E. DuPont de Nemours and Co., The Dow Chemical Co., and the State of Illinois. Use of the APS was supported by the U.S. Department of Energy, Office of Science, Office of Basic Energy Sciences, under Contract DE-AC02-06CH11357. The authors acknowledge Louis Pitet and Mike Bluemle for help with SAXS collection. We also thank Tyler Stack for helping with preliminary oxidation experiments and Frank Bates for helpful suggestions.

■ REFERENCES

(1) Albertsson, A. C.; Varma, I. K. *Adv. Polym. Sci.* **2002**, *157*, 1–40.
(2) Anderson, K. S.; Schreck, K. M.; Hillmyer, M. A. *Polym. Rev.* **2008**, *48*, 85–108.

(3) Lindblad, M. S.; Liu, Y.; Albertsson, A.-C.; Ranucci, E.; Karlsson, S. *Adv. Polym. Sci.* **2000**, *157*, 139–161.
(4) Lim, L. T.; Auras, R.; Rubino, M. *Prog. Polym. Sci.* **2008**, *33* (8), 820–852.
(5) Holden, G.; Kricheldorf, H. R.; Quirk, R. P. *Thermoplastic Elastomers*; Hanser Gardner Publications: Cincinnati, OH, 2004; Vol. 3.
(6) Matsen, M. W.; Thompson, R. B. *J. Chem. Phys.* **1999**, *111* (15), 7139–7146.
(7) Sipos, L.; Zsuga, M.; Deák, G. *Macromol. Rapid Commun.* **1995**, *16* (12), 935–940.
(8) Zhang, S.; Hou, Z.; Gonsalves, K. E. *J. Polym. Sci., Part A: Polym. Chem.* **1996**, *34* (13), 2737–2742.
(9) Frick, E. M.; Zalusky, A. S.; Hillmyer, M. A. *Biomacromolecules* **2003**, *4*, 216–223.
(10) Zhang, Z.; Grijpma, D. W.; Feijen, J. *Macromol. Chem. Phys.* **2004**, *205*, 867–875.
(11) Hiki, S.; Miyamoto, M.; Kimura, Y. *Polymer* **2000**, *41* (20), 7369–7379.
(12) Stridsberg, K.; Albertsson, A.-C. *J. Polym. Sci., Part A: Polym. Chem.* **2000**, *38* (10), 1774–1784.
(13) Shin, J.; Martello, M. T.; Shrestha, M.; Wissinger, J. E.; Tolman, W. B.; Hillmyer, M. A. *Macromolecules* **2011**, *44* (1), 87–94.
(14) Wanamaker, C. L.; Bluemle, M. J.; Pitet, L. M.; O'Leary, L. E.; Tolman, W. B.; Hillmyer, M. A. *Biomacromolecules* **2009**, *10* (10), 2904–2911.
(15) Wanamaker, C. L.; O'Leary, L. E.; Lynd, N. A.; Hillmyer, M. A.; Tolman, W. B. *Biomacromolecules* **2007**, *8* (11), 3634–3640.
(16) Hamley, I. W.; Parras, P.; Castelletto, V.; Castillo, R. V.; Muller, A. J.; Pollet, E.; Dubois, P.; Martin, C. M. *Macromol. Chem. Phys.* **2006**, *207* (11), 941–953.
(17) Muller, A. J.; Balsamo, V.; Arnal, M. L. *Adv. Polym. Sci.* **2005**, *190*, 1–63.
(18) Quiram, D. J.; Register, R. A.; Marchand, G. R. *Macromolecules* **1997**, *30* (16), 4551–4558.
(19) Palmans, A. R. A.; van As, B. A. C.; van Buijtenen, J.; Meijer, E. W. *ACS Symp. Ser.* **2008**, *999*, 230–244.
(20) Breteler, M. R.; Zhong, Z.; Dijkstra, P. J.; Palmans, A. R. A.; Peeters, J.; Feijen, J. *J. Polym. Sci., Part A: Polym. Chem.* **2007**, *45*, 429–436.
(21) Goulet, L.; Prudhomme, R. E. *J. Polym. Sci., Part C: Polym. Sym.* **1990**, *28*, 2329–2352.
(22) Seefried, C. G.; Koleske, J. V. *J. Polym. Sci., Part B: Polym. Phys.* **1975**, *13* (4), 851–856.
(23) van As, B. A. C.; Chan, D.-K.; Kivit, P. J. J.; Palmans, A. R. A.; Meijer, E. W. *Tetrahedron: Asymmetry* **2007**, *18* (6), 787–790.
(24) van As, B. A. C.; van Buijtenen, J.; Heise, A.; Broxterman, Q. B.; Verzijl, G. K. M.; Palmans, A. R. A.; Meijer, E. W. *J. Am. Chem. Soc.* **2005**, *127* (28), 9964–9965.
(25) Vion, J. M.; Jerome, R.; Teyssie, P.; Aubin, M.; Prudhomme, R. E. *Macromolecules* **1986**, *19* (7), 1828–1838.
(26) In a preliminary study, MCL (0.1 mol/L) dissolved in aqueous methanol with sodium bicarbonate led to no appreciable degradation products after 10 h by thin-layer chromatography, indicating the weakly basic solution of sodium bicarbonate is not capable of rapidly hydrolyzing MCL.
(27) Peeters, J.; Palmans, A. R.; Veld, M.; Scheijen, F.; Heise, A.; Meijer, E. W. *Biomacromolecules* **2004**, *5* (5), 1862–1868.
(28) González-Núñez, M. E.; Mello, R.; Olmos, A.; Asensio, G. *J. Org. Chem.* **2005**, *70*, 10879–10882.
(29) González-Núñez, M. E.; Mello, R.; Olmos, A.; Asensio, G. *J. Org. Chem.* **2006**, *71*, 6432–6436.
(30) Kennedy, R. J.; Stock, A. M. *J. Org. Chem.* **1960**, *25*, 1901–1906.
(31) Storey, R. F.; Sherman, J. W. *Macromolecules* **2002**, *35* (5), 1504–1512.
(32) Zhang, D.; Hillmyer, M. A.; Tolman, W. B. *Biomacromolecules* **2005**, *6*, 2091–2095.
(33) Zell, M. T.; Padden, B. E.; Paterick, A. J.; Thakur, K. A. M.; Kean, R. T.; Hillmyer, M. A.; Munson, E. J. *Macromolecules* **2002**, *35* (20), 7700–7707.
(34) Grijpma, D. W.; Pennings, A. J. *Polym. Bull.* **1991**, *25* (3), 335–341.
(35) In'T Veld, P. J. A.; Velner, E. M.; Van de Witte, P.; Hamhuis, J.; Dijkstra, P. J.; Feijen, J. *J. Polym. Sci., Part A: Polym. Chem.* **1997**, *35*, 219–226.
(36) Lynd, N. A.; Hillmyer, M. A. *Macromolecules* **2005**, *38*, 8803–8810.
(37) Anderson, K. S.; Hillmyer, M. A. *Macromolecules* **2004**, *37* (5), 1857–1862.
(38) Cavicchi, K. A.; Lodge, T. P. *J. Polym. Sci., Part B: Polym. Phys.* **2003**, *41* (7), 715–724.
(39) Kim, J. K.; Lee, H. H.; Ree, M.; Lee, K. B.; Park, Y. *Macromol. Chem. Phys.* **1998**, *199* (4), 641–653.
(40) Rosedale, J. H.; Bates, F. S. *Macromolecules* **1990**, *23*, 2329–2338.
(41) Maheshwari, S.; Tsapatsis, M.; Bates, F. S. *Macromolecules* **2007**, *40* (18), 6638–6646.
(42) Hanley, K. J.; Lodge, T. P. *J. Polym. Sci., Part B: Polym. Phys.* **1998**, *36* (17), 3101–3113.
(43) Zalusky, A. S.; Olayo-Valles, R.; Wolf, J. H.; Hillmyer, M. A. *J. Am. Chem. Soc.* **2002**, *124* (43), 12761–12773.
(44) Schmidt, S. C.; Hillmyer, M. A. *J. Polym. Sci., Part B: Polym. Phys.* **2002**, *40* (20), 2364–2376.
(45) Jamshidi, K.; Hyon, S. H.; Ikada, Y. *Polymer* **1988**, *29* (12), 2229–2234.
(46) Krause, S.; Iskandar, M.; Iqbal, M. *Macromolecules* **1982**, *15* (1), 105–111.
(47) Lu, Z.; Krause, S. *Macromolecules* **1982**, *15* (1), 112–114.
(48) Wang, B. Y.; Krause, S. *Macromolecules* **1987**, *20* (9), 2201–2208.
(49) Granger, A. T.; Krause, S.; Fetters, L. J. *Macromolecules* **1987**, *20* (6), 1421–1423.
(50) The ASTM standard test method recommends self-tightening grips were not available for testing these materials.
(51) The tensile behavior of the lower molar mass L−MCL−L triblocks having a PMCL midblock molar mass of 20 kg mol^{-1} were also tested. However, the stress and strain at failure for these triblocks were much lower even with reducing the crosshead velocity and are not reported.
(52) Baeurle, S. A.; Hotta, A.; Gusev, A. A. *Polymer* **2005**, *46* (12), 4344–4354.
(53) Baeurle, S. A.; Hotta, A.; Gusev, A. A. *Polymer* **2006**, *47* (17), 6243–6253.
(54) Rottler, J. *J. Phys.: Condens. Matter* **2009**, *21* (46), 463101–463101.
(55) Tong, J.-D.; Jerome, R. *Macromolecules* **2000**, *33* (5), 1479–1481.
(56) Honeker, C. C.; Thomas, E. L. *Macromolecules* **2000**, *33* (25), 9407–9417.
(57) Honeker, C. C.; Thomas, E. L.; Albalak, R. J.; Hajduk, D. A.; Gruner, S. M.; Capel, M. C. *Macromolecules* **2000**, *33* (25), 9395–9406.
(58) Stasiak, J.; Squires, A. M.; Castelletto, V.; Hamley, I. W.; Moggridge, G. D. *Macromolecules* **2009**, *42* (14), 5256–5265.